Effect of particle size on the activity and durability of the Pt/C electrocatalyst for proton exchange membrane fuel cells

Zhuang Xu[a,b], Huamin Zhang[a,*], Hexiang Zhong[a], Jianlu Zhang[a], Qiuhong Lu[c] and Dangsheng Su[c,d]

[a] R & D Center for Energy Storage, Dalian Institute of Chemical Physics, Chinese Academy of Sciences, Dalian 116023, China
[b] Graduate School of the Chinese Academy of Sciences, Beijing 100039, China
[c] Shenyang National Laboratory of Materials Science, Institute of Metal Research, Chinese Academy of Sciences, Shenyang 110016, China
[d] Fritz Haber Institute of the Max Planck Society, Berlin 14195, Germany

Abstract: In the present investigation, carbon supported Pt with various average particle sizes ranging from sub 3 nm to 6.5 nm were successfully in situ prepared and characterized at the cathode of proton exchange membrane fuel cells. A clear Pt particle size effect on both the oxygen reduction activity and the fuel cell durability of the electrocatalyst was revealed. As Pt particle size increases, both the oxygen reduction specific activity and the electrochemical stability are improved. However, the mass activity of Pt is balanced by the electrochemical surface area loss, with around 4.5 nm be optimal. For Pt mean particle size growing from 2.9 nm to 3.5 nm, a sharp enhancement of the electrochemical stability was observed. The reduced occupation of corner and edge atoms on the Pt surface is believed has weaken the adsorption of the oxygenated species on Pt, and thereafter releases more available active sites for oxygen reduction and also renders the Pt surface a stronger resistance against potential cycling. It is therefore proposed that by designing the Pt microstructure with more face atoms on the surface, cathode electrocatalyst with both improved activity and enhanced durability would be developed for proton exchange membrane fuel cells.

Keywords: Proton exchange membrane fuel cells, Pt/C electrocatalyst, particle size, activity, durability

1. Introduction

Proton exchange membrane fuel cells (PEMFCs) have been considered as the ideal energy conversion devices for mobile and stationary applications because of their high efficiency, high power density, fast response, low temperature operation, and zero emission [1]. Carbon supported Pt is generally adopted as the electrocatalyst for the oxygen reduction reaction (ORR) at the cathode and the hydrogen reduction reaction (HOR) at the anode in PEMFCs. Due to the sluggish kinetics of the ORR [2, 3], a high Pt loading is normally required to maintain the desirable cell performance, resulting in a high cost of PEMFCs which hinders their commercialization [4]. To address this issue, reducing the size of Pt particles immobilized on the carbon support is favored [5-8]. Since Pt particles with smaller sizes expose a higher ratio of surface atoms, an increased utilization of Pt can be achieved. However, as the nano-scaled Pt works under harsh conditions, especially at the PEMFC cathode with high temperature, low pH, high relative humidity, fluctuant potential and an oxygen atmosphere, Pt particles with smaller sizes are more apt to grow and lose surface area, leading to the durability concern of PEMFCs [9-13]. Therefore, Pt particle size is one of the key factors that determine both the electrocatalytic activity and the durability of carbon supported Pt electrocatalysts used in PEMFCs.

Up to now, there still remains a debate on the effect of Pt particle size on the activity for ORR. Several works reported that Pt reached the maximum mass activity at 3-5 nm [14-17], while others observed a straight increase of mass activity as Pt particle size decreased [18-20]. Penckert et al. [14], for instance, found that the ORR specific activity was constant with Pt particle sizes above 4 nm but it dropped by a factor of 20 when the particle size decreased from 3 nm to 1 nm, suggesting around 4 nm be the optimum Pt particle size for the maximum ORR mass activity. By depositing Pt on high surface area carbons, Watanane et al. [18], however,

demonstrated a constant ORR specific activity when Pt particle size deceased to even 1.4 nm, indicating there was no Pt particle size effect on catalyzing the ORR. These contradictory results probably stem from the various catalyst preparation processes and activity evaluation methodologies. Although there are studies introducing stabilizing agents to prepare carbon supported Pt with various average sizes [16, 21], the influence of the surfactant, ligand, or polymer on the electrocatalyst activity should be taken into consideration. Also, since most of the previous activity measurements were carried out in a sulfuric acid electrolyte, the selective adsorption of (bi)sulfate anion on Pt surface [22, 23] might lead to a different trend to that under the practical PEMFC operating conditions. For the Pt particle size effect on the electrocatalyst durability in PEMFCs, however, fewer studies have been reported. Matsutani et al. [24] observed an improved stability of Pt against PEMFC load cycling as the Pt particle size increased from 2-3 nm to 4-5 nm after heat treatment, but detailed mechanism for the stability improvement was not addressed. Based on the literature, a comprehensive investigation with well-defined preparation and evaluation methodology regarding Pt particle size effect on the activity for ORR and the durability of Pt/C in PEMFCs is yet to be conducted.

In this study, instead of chemically depositing Pt on carbon support, a series of carbon supported Pt with increasing average particle sizes ranging from sub 3 nm to 6.5 nm were prepared by an electrochemical aging method. Compared to the previous methodologies, this preparation allows in situ monitoring of the Pt particle size effect on the activity and durability of Pt/C electrocatalyst in PEMFCs. Based on the efficient preparation and in situ measurements, mechanism for the Pt particle size effect was investigated, and a reasonable scheme to improve the activity and durability of Pt/C in PEMFCs was also proposed.

2. Experimental

2.1. Electrocatalyst preparation

Electrocatalysts with various average Pt particle sizes were prepared by electrochemically aging identical pristine Pt/C for various durations in a single cell.

The details are as follows: Homogeneous catalyst inks, obtained by mixing 46.2 wt% Pt/C (TKK Corp.) with 5 wt% Nafion$^{\circ,R}$ ionomer solution (DuPont) and isopropanol in an ultrasonic bath, were sprayed onto the poly(tetrafluoroethylene) hydrophobilized carbon papers (Cabot Corp.) to form the gas diffusion electrodes (GDEs). The Pt loadings were controlled at 0.3 mg cm^{-2} and 0.7 mg cm^{-2} and the dry Nafion$^{\circ,R}$ loadings were controlled at 0.3 mg cm^{-2} and 0.5 mg cm^{-2} for anodic and cathodic catalyst layers, respectively. Then, membrane electrode assemblies (MEAs) with an active area of 5 cm^2 were fabricated by hot-pressing Nafion$^{\circ,R}$ 212 membranes (DuPont) sandwiched between the two identical electrodes at 1 MPa and 140 □ for 1 min. Using the as-prepared MEAs, single PEMFCs were assembled, submitted to the house-made test station, and conditioned for at least 8 h until a reproducible cell performance was achieved. Single cells were operated at 80 □ with anodic hydrogen (0.2 MPa) and cathodic oxygen (0.2 MPa) streams pre-humidified through their respective water-bubblers at 90 □ and 85 □. After that, the cathodic oxygen was switched to pure nitrogen with the identical back pressure and relative humidity. With the open circuit voltage dropping to below 0.100 V, the nitrogen electrode was subjected to a cyclic voltammetry (CV) cycling on a CHI 600B electrochemical station (CH Instruments). During the CV aging, the dynamic hydrogen electrode (DHE) [25] functioned as both the reference and the counter electrodes, and the CVs were profiled between 0.6 V and 1.2 V vs. DHE at a scan rate of 50 mV s^{-1}. Electrocatalysts obtained after various numbers of CVs, e.g. 0, 300, 800, 1500, 2400, 3500, and 4800, were named as EA0, EA300, EA800, EA1500, EA2400, and EA 3500, respectively.

2.2. Physical characterization

The morphology of the as-prepared electrocatalysts was observed on a TCNAI 20 G2 transmission electron microscope (TEM). The samples were obtained by scrapping from the cathodic catalyst layers of the disassembled MEAs. Each sample was suspended in ethanol by ultrasonicating to form a homogeneous slurry. A drop of the slurry was then casted onto the carbon-coated copper grid followed by solvent

evaporation in vacuum at 60 ℃. In order to determine the Pt particle size distribution of each electrocatalyst, three hundred Pt particles randomly chosen from at least three different regions were analyzed.

2.3. Electrochemical characterization

Electrochemical measurements of the as-prepared electrocatalysts at cathode were carried out on the CHI 600B electrochemical station (CH Instruments). The DHE served as both the reference and the counter electrodes, and the cell temperature was controlled at 80 ℃. Several cycles of CVs were first conducted to obtain a stable and reproducible profile. After that, cyclic voltammogram was recorded in a potential window of 0 V to 1 V vs. DHE with a scan rate of 20 mV s^{-1}.

2.4. Activity and durability evaluations

ORR activities of the as-prepared electrocatalysts were in situ monitored adopting the methodology proposed by Gasteiger et al [4]. After each electrochemical aging process, the H_2-crossover of the MEA was evaluated by the diffusion-limited current density of hydrogen oxidation at 0.4 V vs. DHE in the linear sweep voltammetry (LSV) [26]. The LSV was profiled from 0 V to 1 V vs. DHE with a scan rate of 5 mV s^{-1}. Then, the cathodic atmosphere was switched to oxygen and the cell was conditioned to a stable performance. Polarization curves as well as the internal cell resistance R (at 10 kHz) were measured on a KFM2030 (Kikusui Electronics Corp.) fuel cell meter. The mass activity (in units of A mg^{-1}_{Pt}) of the electrocatalyst towards the ORR in PEMFC was calculated via dividing the H_2-crossover calibrated cell current density at the IR-free cell voltage (the cell voltage was calibrated by adding the voltage drop caused by the internal cell resistance) of 0.9 V [4] by the Pt loading, and the specific activity (in units of μA cm^{-2}_{Pt}) was obtained via dividing the mass activity by the corresponding electrochemical surface area (ESA) of the electrocatalyst.

In order to evaluate the electrocatalyst durability, after the activity measurements, as-prepared electrocatalysts EA0, EA300, EA800, EA1500, EA2400, and EA3500

were respectively subjected to 300, 500, 700, 900, 1100 and 1300 cycles of driven potential cycling in the range of 0.6 V to 1.2 V vs. DHE with a scan rate of 50 mV s^{-1}. The single cell setup was the same as that during the electrochemical aging process. ESA loss per cycle was calculated and used to estimate the durability of the electrocatalyst at PEMFC cathode.

3. Results and Discussion

3.1. Pt particle size and electrochemical surface area

Fig. 1 presents typical TEM images of the as-prepared electrocatalysts. For both the pristine and the electrochemically aged electrocatalysts, Pt nanoparticles are well dispersed on the carbon support. After electrochemical aging, the Pt particles grow in size. However, few agglomerations are observed. Based on the measurements of 300 particles selected from random regions, the distributions of Pt particle sizes for different electrocatalysts are depicted in Fig. 2. It is observed that by prolonging the duration of electrochemical aging, the mean size of Pt particles increases from 2.9 nm to 6.5 nm, while the relatively narrow Pt particle size distribution is reserved. These results clearly demonstrate that the electrochemical aging method is quite effective in preparing electrocatalysts with various mean Pt particle sizes.

The change of the electrochemical surface areas (ESAs, in units of $m^2\ g^{-1}_{Pt}$) for the as-prepared electrocatalysts is displayed in Fig. 3. The ESAs were estimated from the hydrogen desorption charge integrated from the relevant potential region according to the in situ cyclic voltammograms [27]. The calculation was performed assuming 210 μC cm^{-2} as the specific capacity for the hydrogen desorption reaction on Pt [27], with correction of the double layer coulombs. All the ESAs are normalized by the value of the pristine electrocatalyst EA0 to give a clear comparison. As can be seen, the normalized ESA of the Pt/C electrocatalyst decreases with the increase of the mean Pt particle size. For a controlled Pt loading and a narrow Pt particle size distribution, the overall surface area of spherical Pt particles in the catalyst layer can be estimated through the equation

$$S = \frac{6m}{\rho \bar{d}_n} \tag{1}$$

where m and ρ are the mass and the density of Pt and $\bar{d}_n$ is the average diameter of Pt particles. According to this equation, the overall surface area of Pt in the catalyst layer should be inversely proportional to the Pt average diameter (particle size). This trend is also observed for the ESAs of the as-prepared electrocatalysts (indicated by the red dashed line in Fig. 3). Therefore, it is inferred that the ratio of the electrocatalyst ESA to the overall Pt surface area, which is referred to as the utilization of Pt in the catalyst layer [4], should be similar among the as-prepared electrocatalysts.

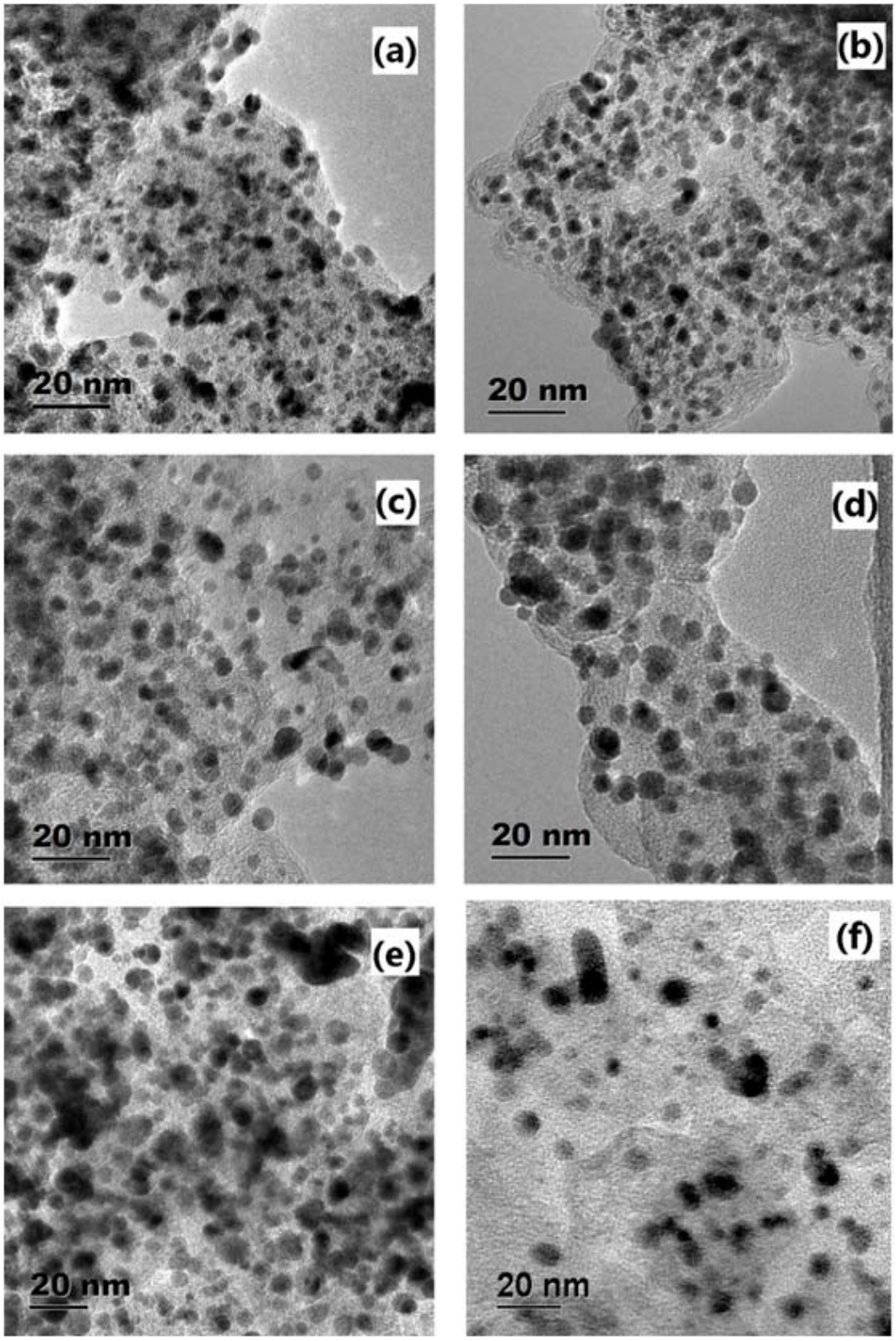

Fig. 1. Typical TEM images of electrocatalysts EA0 (a), EA300 (b), EA800(c), EA1500 (d), EA2400 (e), and EA3500 (f).

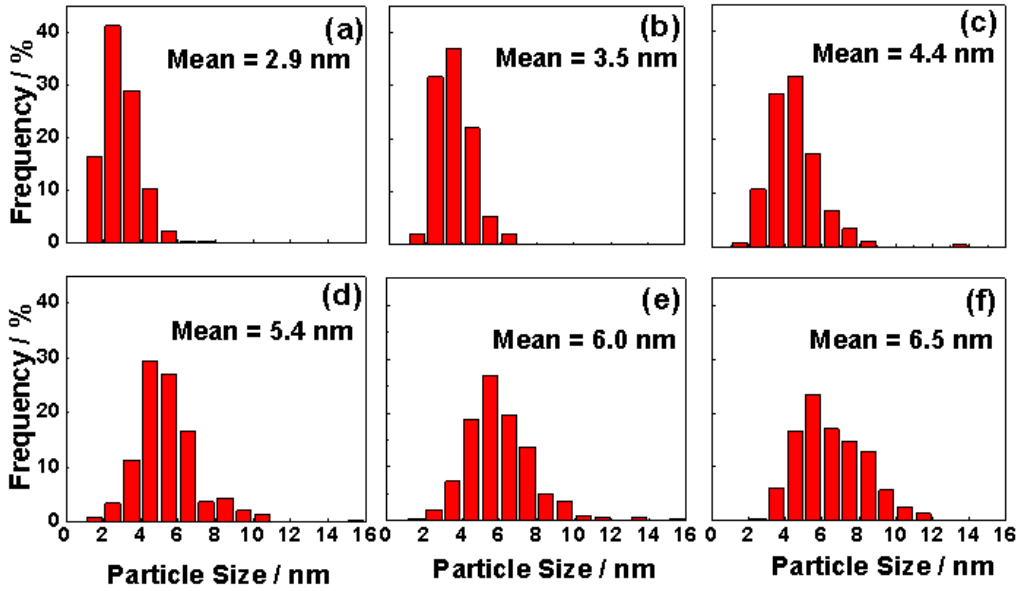

Fig. 2. Histograms of Pt particle size distributions for electrocatalysts EA0 (a), EA300 (b), EA800(c), EA1500 (d), EA2400 (e), and EA3500 (f).

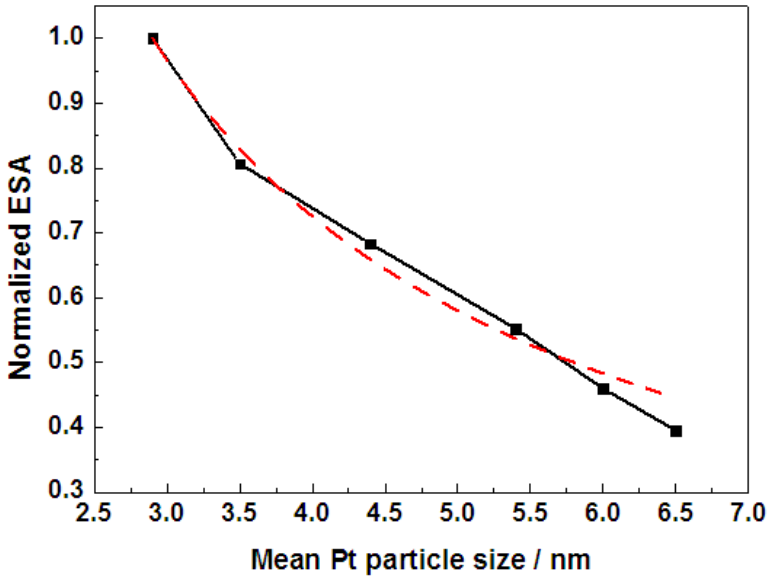

Fig. 3. Normalized electrochemical surface area of carbon supported Pt electrocatalyst as a function of the mean Pt particle size.

3.2. Oxygen reduction activity

In order to monitor the Pt particle size effect on the activity for ORR, the as-prepared electrocatalysts at cathode were evaluated by measuring polarization curves. The cell current densities were corrected by the current densities caused by hydrogen crossover and the cell voltages were calibrated by the potential drops caused

by cell internal resistances as well [4]. The kinetic characteristics of the electrocatalysts are compared in Fig. 4. Clearly, electrocatalysts EA300 and EA800 are more active towards the ORR than EA0, which suggests that increasing mean Pt particle size from 2.9 nm to 4.4 nm did not cause an activity loss. Even for electrocatalyst EA1500 with a mean Pt particle size of 5.4 nm, the oxygen reduction activity is comparable to that of EA0. Further increasing Pt particle size to beyond 5.4 nm, as for electrocatalysts EA2400 and EA3500, however, leads to an activity loss. These results indicate that the activity of Pt towards the ORR is related to the Pt particle size and there is an optimum Pt particle size for the electrocatalyst.

Fig. 5 depicts the change of the ORR mass activity for the Pt/C electrocatalyst against the mean particle size of Pt. The ORR mass activity was determined via dividing the hydrogen-crossover corrected cell current density at the iR-free cell voltage of 0.9V by the Pt loading in the catalyst layer [4], according to the polarization curves in Fig. 4. All the mass activities are normalized by the value of electrocatalyst EA0. It is obvious that the mass activity of Pt/C reaches the maximum value when Pt particle size falls around 4.4 nm, while it decreases when the Pt particle size is below 3.5 nm or above 5.4 nm. Since the ESA vanishes as Pt particle size increases (see Fig. 3), this mass activity change feature indicates that the ORR specific activity is not constant among the as-prepared Pt/C electrocatalysts.

Calculated via dividing the mass activity by the ESA, the ORR specific activities for the electrocatalysts are displayed in Fig. 5. A continuous improvement of specific activity is observed as Pt particle size grows from 2.9 nm to 6.5 nm. As shown, the specific activity of electrocatalyst EA3500 with a mean Pt particle size of 6.5 nm is about 1.8 times that of electrocatalyst EA0 with a mean Pt particle size of 2.9 nm. For an increased Pt particle size, this improved specific activity balances the mass activity change caused by the ESA loss of the electrocatalyst. Compared to electrocatalyst EA0, although the ESAs of electrocatalysts EA300 and EA800 are lower, the enhanced specific activities are able to compensate the mass activity loss caused by the ESA loss, and therefore lead to improved mass activities. However, when the mean Pt particle size exceeds 5.4 nm, the ESA is outstandingly low (less

than 60% of the pristine), and the specific activity improvement fails to make up the mass activity drop caused by the ESA loss. As a result, the mass activities of electrocatalysts EA1500, EA2400, and EA3500 are lower than that of electrocatalyst EA0.

To further investigate the Pt particle size effect on the ORR specific activity, cyclic voltammogram was recorded for each as-prepared electrocatalyst at cathode, and the results are presented in Fig. 6. As the Pt particle size increases from 2.9 nm (electrocatalyst EA0) to 6.5 nm (electrocatalyst EA3500), the current intensity decreases for the peaks of both the hydrogen desorption and the Pt-O_x reduction, indicating the reduction in the ESA. Furthermore, intensity ratio of Peak A to Peak B alters in the hydrogen desorption region, and the Pt-O_x reduction peak (Peak C) potential also shifts among the electrocatalysts. Compared to electrocatalyst EA0 with a mean Pt size of 2.9 nm, the occupation of Peak A for electrocatalyst EA3500 with a mean Pt size of 6.5 nm decreases, suggesting a reduced fraction of the edge and corner atoms (defects) on the Pt surface [28, 29]. This surface modification derived from the Pt particle size change is believed to result in the ORR specific activity enhancement. Because the defect atoms possess a strong affinity to oxygen containing species (e.g. hydroxyl), nanometer sized Pt particles with high fraction of defects are easily blocked at the surface by the oxygenated adsorbates generated during the ORR [30-32]. For Pt with increased particle size, as confirmed by the positive shift of the Pt-O_x reduction potential, the reduced defects occupation alleviates the surface blocking effect, release more available electrocatalytic sites, and therefore results in an improved specific activity for the Pt/C electrocatalyst.

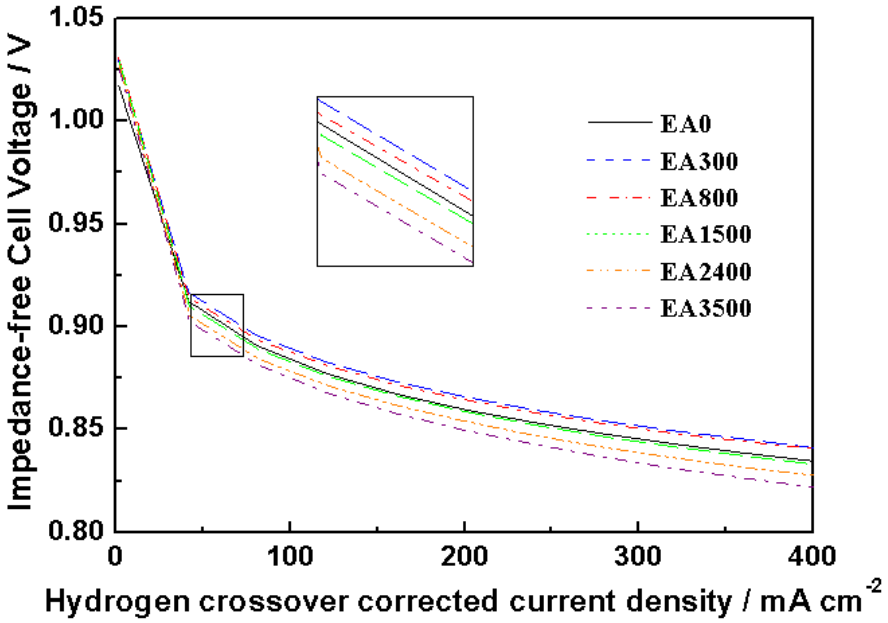

Fig. 4. Polarization curves of single cell adopting as-prepared Pt/C electrocatalysts at cathode. The current densities are corrected with the values caused by hydrogen crossover and the cell voltages are IR- free.

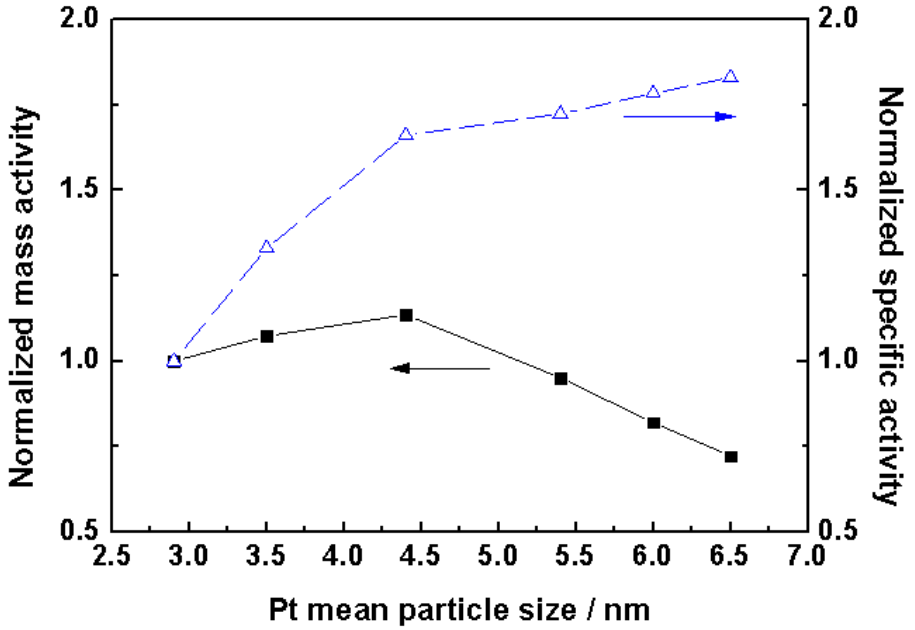

Fig. 5. Mass activities and specific activities for Pt/C electrocatalysts with various mean Pt particle sizes. All the values are normalized to that of the pristine electrocatalyst EA0.

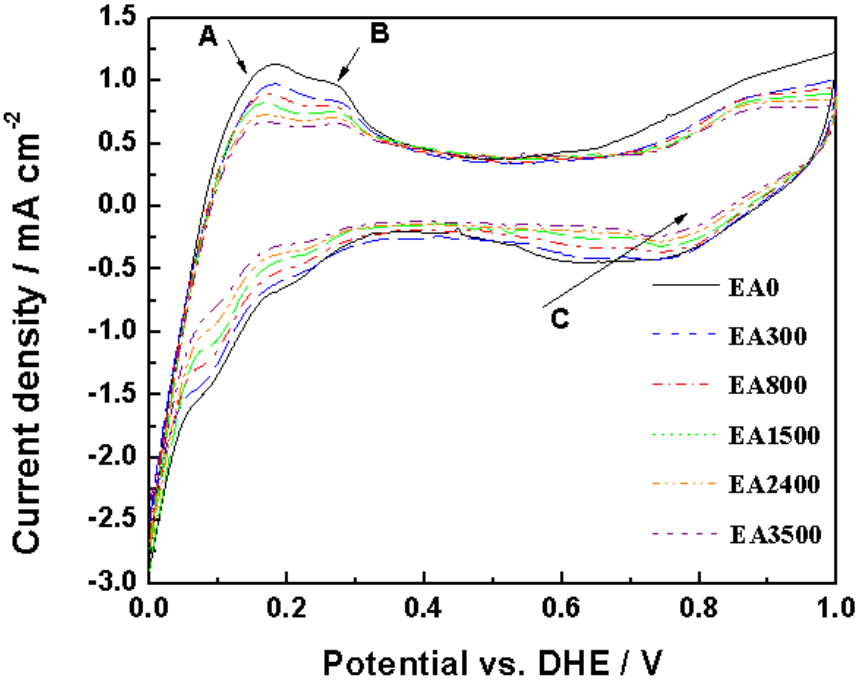

Fig. 6. In situ cyclic voltammograms of as-prepared Pt/C electrocatalysts. Scan rate: 20mV s^{-1}.

3.3. Fuel cell durability

Accelerated stress test (AST) based on potential cycling was employed to assess the electrochemical stability for the Pt/C electrocatalysts with various mean Pt particle sizes. The AST has been proven an effective method [33-35], since it accelerates the degradation rate of the electrocatalyst in fuel cell while affects other components (e.g. the proton exchange membrane) little. Considering the practical PEMFC working conditions, the potential window for the AST is chosen 0.6-1.2 V vs. DHE. The Pt/C electrocatalysts at cathode are subjected to programmed durations of potential cycling in order to obtain a similar ESA loss percentage. To evaluate the durability of the electrocatalyst, the ESA loss rate (percentage of ESA loss per cycle) during the AST is calculated according to the following equation:

$$r_{ESA}[percentage/cycle] = \frac{ESA_{before} - ESA_{after}}{ESA_{before} \times N_{cycle}} \quad (2)$$

where N_{cycle} represents the cycling number in AST. As depicted in Fig. 7, the ESA loss rate diminishes as the mean Pt particle size increases, indicating that Pt/C

electrocatalsyt with a larger Pt particle size shows a better electrochemical stability at PEMFC cathode. With the Pt particle size increase from 2.9 to 3.5 nm, the ESA loss rate encounters a sharp decrease from 0.064 % per cycle to 0.031 % per cycle, while it exhibits a comparable ESA loss rate when the particle size increased from 3.5 to 4.5 nm. Further enlarging the Pt particle size leads to a continuous decrease in the ESA loss rate against potential cycling. For electrocatalyst EA3500 with a mean Pt particle size of 6.5 nm, the ESA loss rate reaches as low as 0.003 % per cycle.

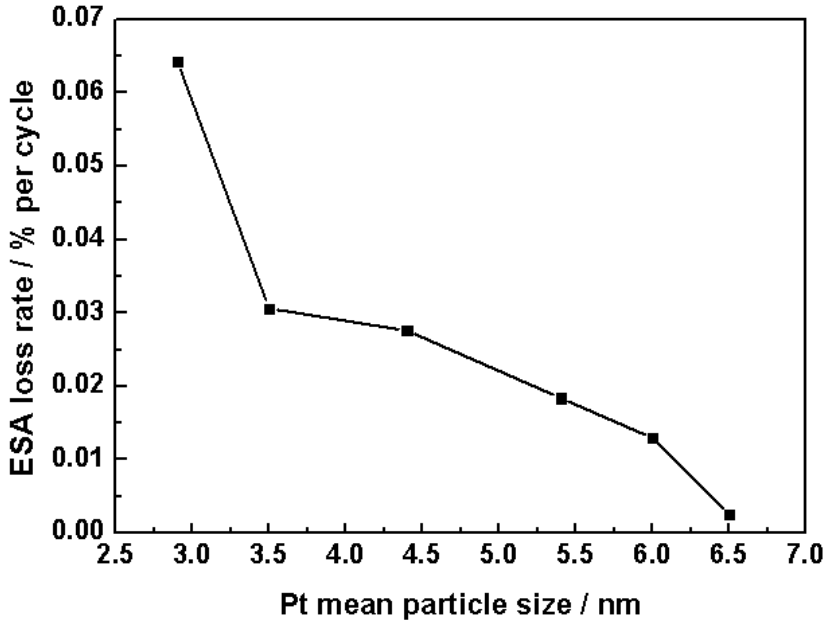

Fig. 7. ESA loss rates during accelerated stress test for Pt/C electrocatalysts with various mean Pt particle sizes.

As small particles possess high surface-area-to-volume ratio, they tend to grow to lower their surface free energy [36, 37]. On the other hand, under potential cycling, Pt particles encounter a Pt dissolution/re-deposition process [7, 38, 39]. During the positive scan, Pt surface atoms are oxidized and some of them dissolve into the electrolyte, while at the negative scan the surface atoms are reduced and the Pt ions re-deposit onto the surface [7, 38, 39]. Since the atoms at edges and corners (defects) on the Pt surface are low coordinated, they have strong affinity to oxygenated species generated in the electrode reaction, and they are more apt to undergo the Pt

dissolution process compared to the face atoms. For Pt particles less than 3 nm, the defects fraction on the surface is rather high [15, 40], adding to an extra surface free energy, and the surface has a strong tendency to lower its energy through particle size growth (surface area reduction) and defect diminishing. Therefore, electrocatalyst EA0 with 2.9 nm mean Pt particle size demonstrates a high ESA loss rate in the AST. For electrocatalyst EA300 with 3.5 nm mean Pt particle size, the dramatic reduce in ESA loss rate is believed to be due to the surface modification in the preparation procedure. Previous electrochemical aging is considered has facilitated the reduction of the defects on the Pt surface by enlarging the particle size and reconstructing the surface with fewer defects. This process is reflected by the decreased response current of hydrogen desorption and the reduced intensity ratio of Peak A to B in the in situ cyclic voltammogram presented in Fig. 6. Further enlarging Pt particle size over 3.5 nm continues to result in the decrease of ESA loss rate. It is interesting that after the sharp decrease, the degradation of the ESA loss rate slows down a lot. This effect is probably caused by the substantial reduction of the Pt particles less than 2 nm, according to the particle size distributions in Fig. 2. As shown, from electrocatalyst EA0 to electrocatalyst EA300, the occupation of the sub 2 nm Pt particles almost vanishes. The degradation of the ESA loss rate after mean Pt particle size exceeding 3.5 nm is believed to be due to the reduction of the surface-area-to-volume ratio and the surface defects occupation. The ESA loss rate finally reaches a rather small value when the mean Pt particle size increased to 6.5 nm. Therefore, it is expected that the Pt particles below 3 nm possess a rather poor electrochemical stability than that with the particle size of 3.5 nm or above. On the other hand, Pt particles with lower fractions of defects on the surface would demonstrate a better durability in PEMFCs as well.

3.4. Pt particle size effect

The particle size effect on the oxygen reduction activity and electrochemical durability for Pt/C electrocatalyst in PEMFCs is believed to be due to the Pt surface modification during the particle size change. Besides the surface area, which

decreases with the particle size increase, the Pt surface conformation is another important factor that influences the activity and durability of Pt/C electrocatalyst. To simulate the particle size effect on the surface structure change, fractions of face atoms and defects on the surface versus particle size was calculated for the cuboctahedron Pt nanoparticles, according to the model proposed by Van Hardeveld et al [40]. The cuboctahedron model is chosen because of its theoretical stability and analogous structure to practical Pt/C electrocatalysts [17, 41]. The simulation curves and the typical high resolution TEM image of electrocatalyst EA3500 are shown in Fig. 8. As illustrated in the curves, fraction of defects decreases with Pt diameter increase. This change reduces the adsorption of the oxygenated species on the surface, which is believed to block the active sites for catalyzing oxygen reduction [2, 3], and therefore the specific activity of Pt improves. However, the reduction of the defects fraction on the surface is synchronized with the decrease of Pt surface area (or ESA), and then these two different factors result in an optimal Pt particle size (around 4.4nm in this study) with which the electrocatalyst reaches the maximum mass activity.

For the electrocatalyst durability in PEMFCs, the Pt particle size effect is rather straight. Because both the particle size growth (ESA decrease) and the defect diminishing lead to the reduction in surface free energy, the electrochemical stability is improved as Pt particle size increases. A remarkable effect is the sharp increase of the Pt stability against potential cycling when the mean particle size exceeds 3 nm. The different trends of Pt particle size effect on the mass activity and electrochemical stability bring about a necessary trade-off in determining the optimal Pt particle size for the electrocatalyst in PEMFCs. According to the present investigation, Pt particle sizes of around 4.4 nm are considered to be optimal for the activity and durability of Pt/C electrocatalyst in PEMFCs.

In addition, it is notable that the reduction of defects fraction on the Pt surface improves both the ORR specific activity and the electrochemical stability of the electrocatalyst. If the defects reduction could be separated from the ESA decrease, it is possible to improve the mass activity as well. Therefore, designing and synthesizing Pt microstructures with high fraction of face atoms on the surface is thought to be one

probable strategy to obtain Pt/C electrocatalyst with both enhanced activity and better durability for PEMFC cathode.

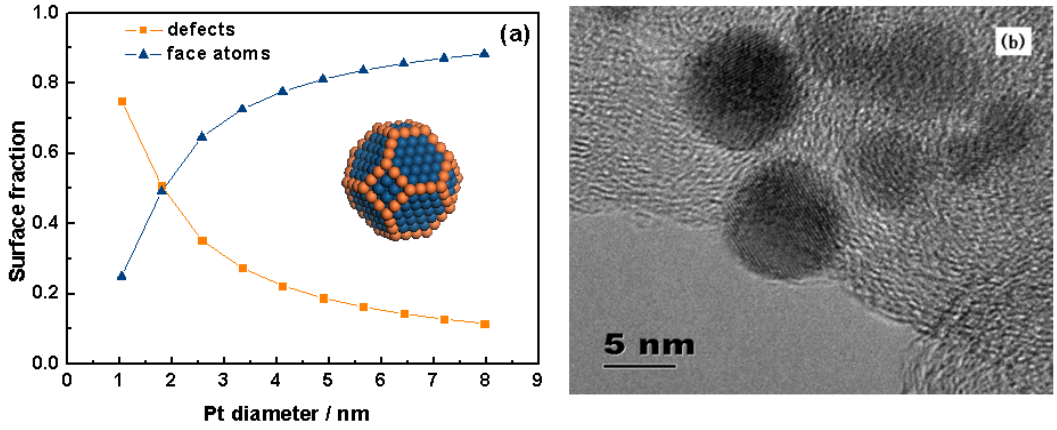

Fig. 8. (a) Surface simulation for cuboctahedral Pt nanoparticles with various diameters; (b) Typical high resolution TEM image of the electrocatalyst EA3500.

4. Conclusions

In the present work, Pt/C electrocatalysts with mean particle sizes ranging from 2.9 nm to 6.5 nm have been successfully prepared via an electrochemical aging method and evaluated in situ as cathodic electrocatalyst in PEMFCs. The Pt nanoparticles showed a clear particle size effect on the oxygen reduction activity and the electrochemical stability for the electrocatalyst. The reduction of surface defects during the particle size increase alleviates the strong adsorption of oxygenated species on the Pt surface, resulting in both an improved ORR specific activity and a better electrochemical stability for Pt/C electrocatalysts. However, the simultaneous ESA loss with the particle size increase reduces the utilization of Pt atoms, and the ORR mass activity is balanced with a maximum value when Pt particle size falls around 4.4 nm. Therefore, it is proposed that via a reasonable design of the Pt microstructure with a higher fraction of face atoms on the surface, PEMFC cathode Pt/C electrocatalysts with both enhanced mass activity and durability would be obtained.

Acknowledgements

The authors appreciate the financial support from the National High Technology Research and Development Program of China (2009AA05Z114 and 2008AA05Z106).

Reference

[1] J. Larminie, A. Dicks, Fuel Cell Systmes Explained, Second Edition ed., John Wiley & Sons Ltd., Chichester, 2003.

[2] J.K. Norskov, J. Rossmeisl, A. Logadottir, L. Lindqvist, J.R. Kitchin, T. Bligaard, H. Jonsson, J. Phys. Chem. B 108 (2004) 17886-17892.

[3] V.R. Stamenkovic, B. Fowler, B.S. Mun, G.F. Wang, P.N. Ross, C.A. Lucas, N.M. Markovic, Science 315 (2007) 493-497.

[4] H.A. Gasteiger, S.S. Kocha, B. Sompalli, F.T. Wagner, Appl. Catal. B-Environ. 56 (2005) 9-35.

[5] T. Yoshitake, Y. Shimakawa, S. Kuroshima, H. Kimura, T. Ichihashi, Y. Kubo, D. Kasuya, K. Takahashi, F. Kokai, M. Yudasaka, S. Iijima, Physica B 323 (2002) 124-126.

[6] H.S. Oh, J.G. Oh, Y.G. Hong, H.S. Kim, Electrochim. Acta 52 (2007) 7278-7285.

[7] P.J. Ferreira, G.J. la O, Y. Shao-Horn, D. Morgan, R. Makharia, S. Kocha, H.A. Gasteiger, Journal of the Electrochemical Society 152 (2005) A2256-A2271.

[8] S. Song, Y. Liang, Z. Li, Y. Wang, R. Fu, D. Wu, P. Tsiakaras, Applied Catalysis B: Environmental 98 (2010) 132-137.

[9] S.Y. Huang, P. Ganesan, B.N. Popov, Appl. Catal. B-Environ. 102 (2011) 71-77.

[10] Y.Y. Shao, G.P. Yin, Y.Z. Gao, Journal of Power Sources 171 (2007) 558-566.

[11] J. Xie, D.L. Wood, D.M. Wayne, T.A. Zawodzinski, P. Atanassov, R.L. Borup, Journal of the Electrochemical Society 152 (2005) A104-A113.

[12] J. Xie, D.L. Wood, K.L. More, P. Atanassov, R.L. Borup, Journal of the Electrochemical Society 152 (2005) A1011-A1020.

[13] M.S. Wilson, F.H. Garzon, K.E. Sickafus, S. Gottesfeld, Journal of the Electrochemical Society 140 (1993) 2872-2877.

[14] M. Peuckert, T. Yoneda, R.A.D. Betta, M. Boudart, Journal of the Electrochemical Society 133 (1986) 944-947.

[15] K. Kinoshita, Journal of the Electrochemical Society 137 (1990) 845-848.

[16] K. Wikander, H. Ekstrom, A. Palmqvist, G. Lindbergh, Electrochim. Acta 52 (2007) 6848-6855.

[17] M.L. Sattler, P.N. Ross, Ultramicroscopy 20 (1986) 21-28.

[18] M. Watanabe, S. Saegusa, P. Stonehart, Chemistry Letters (1988) 1487-1490.

[19] J. Bett, Lundquis.J, Electrochim. Acta 18 (1973) 343-348.

[20] L.J. Bregoli, Electrochim. Acta 23 (1978) 489-492.

[21] C.V. Rao, B. Viswanathan, The Journal of Physical Chemistry C 114 (2010) 8661-8667.

[22] N. Markovic, H. Gasteiger, P.N. Ross, Journal of the Electrochemical Society 144 (1997) 1591-1597.

[23] N.M. Markovic, H.A. Gasteiger, P.N. Ross, The Journal of Physical Chemistry 99 (1995) 3411-3415.

[24] K. Matsutani, K. Hayakawa, T. Tada, Platinum Metals Review 54 (2010) 223-232.

[25] G.C. Li, P.G. Pickup, Electrochim. Acta 49 (2004) 4119-4126.

[26] M. Inaba, T. Kinumoto, M. Kiriake, R. Umebayashi, A. Tasaka, Z. Ogumi, Electrochim. Acta 51 (2006) 5746-5753.

[27] A. Pozio, M. De Francesco, A. Cemmi, F. Cardellini, L. Giorgi, Journal of Power Sources 105 (2002) 13-19.
[28] G.A. Attard, J.E. Gillies, C.A. Harris, D.J. Jenkins, P. Johnston, M.A. Price, D.J. Watson, P.B. Wells, Applied Catalysis A: General 222 (2001) 393-405.
[29] J. Solla-Gullón, P. Rodríguez, E. Herrero, A. Aldaz, J.M. Feliu, Physical Chemistry Chemical Physics 10 (2008) 1359.
[30] O. Antoine, Y. Bultel, R. Durand, Journal of Electroanalytical Chemistry 499 (2001) 85-94.
[31] V. Stamenković, T.J. Schmidt, P.N. Ross, N.M. Marković, The Journal of Physical Chemistry B 106 (2002) 11970-11979.
[32] A.S. Aricò, A. Stassi, E. Modica, R. Ornelas, I. Gatto, E. Passalacqua, V. Antonucci, Journal of Power Sources 178 (2008) 525-536.
[33] R.L. Borup, J.R. Davey, F.H. Garzon, D.L. Wood, M.A. Inbody, Journal of Power Sources 163 (2006) 76-81.
[34] K. Yasuda, A. Taniguchi, T. Akita, T. Ioroi, Z. Siroma, Physical Chemistry Chemical Physics 8 (2006) 746-752.
[35] S.S. Zhang, X.Z. Yuan, H.J. Wang, W. Merida, H. Zhu, J. Shen, S.H. Wu, J.J. Zhang, Int. J. Hydrog. Energy 34 (2009) 388-404.
[36] L.Q. Yang, A.E. Depristo, J. Catal. 149 (1994) 223-228.
[37] Y. Shao-Horn, W.C. Sheng, S. Chen, P.J. Ferreira, E.F. Holby, D. Morgan, Topics in Catalysis 46 (2007) 285-305.
[38] R.M. Darling, J.P. Meyers, Journal of the Electrochemical Society 150 (2003) A1523-A1527.
[39] Y.Y. Shao, G.P. Yin, Y.Z. Gao, P.F. Shi, Journal of the Electrochemical Society 153 (2006) A1093-A1097.
[40] R. Van Hardeveld, F. Hartog, Surface Science 15 (1969) 189-230.
[41] N. Semagina, L. Kiwi-Minsker, Catalysis Reviews: Science and Engineering 51 (2009) 147 - 217.